Altered Extracellular Matrix Remodeling and Angiogenesis in Sponge Granulomas of Thrombospondin 2-Null Mice

Themis R. Kyriakides,* Yu-Hong Zhu,*
Zhantao Yang,* Grace Huynh,* and
Paul Bornstein*†

From the Departments of Biochemistry* and Medicine,†
University of Washington, Seattle, Washington

The matricellular angiogenesis inhibitor, thrombospondin (TSP) 2, has been shown to be an important modulator of wound healing and the foreign body response. Specifically, TSP2-null mice display improved healing with minimal scarring and form well-vascularized foreign body capsules. In this study we performed subcutaneous implantation of sponges and investigated the resulting angiogenic and fibrogenic responses. Histological and immunohistochemical analysis of sponges, excised at 7, 14, and 21 days after implantation, revealed significant differences between TSP2-null and wild-type mice. Most notably, TSP2-null mice exhibited increased angiogenesis and fibrotic encapsulation of the sponge. However, invasion of dense tissue was compromised, even though its overall density was increased. Furthermore, histomorphometry and biochemical assays demonstrated a significant increase in the extracellular distribution of matrix metalloproteinase (MMP) 2, but no change in the levels of active transforming growth factor-β_1. The alterations in neovascularization, dense tissue invasion, and MMP2 in TSP2-null mice coincided with the deposition of TSP2 in the extracellular matrix of wild-type animals. These observations support the proposed role of TSP2 as a modulator of angiogenesis and matrix remodeling during tissue repair. In addition, they provide *in vivo* evidence for a newly proposed function of TSP2 as a modulator of extracellular MMP2 levels.   (Am J Pathol 2001, 159:1255–1262)

Thrombospondin (TSP) 2 is a secreted, modular, extracellular matrix (ECM) glycoprotein that functions as a modulator of cell-matrix interactions.[1,2] Mainly recognized as a naturally occurring potent inhibitor of angiogenesis, TSP2 has also been shown to modulate fibroblast adhesion, bone formation, and hemostasis.[3–5] Recent studies have demonstrated that the lack of TSP2 can have profound effects on tissue repair and regeneration processes. Specifically, TSP2-null mice were shown

to heal at an accelerated rate and with reduced scarring.[6] These alterations were associated with prolonged wound neovascularization, increased cellularity, and disorganized ECM deposition. Moreover, analysis of the foreign body response (FBR) in these mice revealed similar alterations, involving mainly the angiogenic and fibrogenic response.[7] However, wound healing and the FBR despite many similarities, including the formation of new tissue, are distinct responses. Thus, unlike wound healing, in which damaged tissue is re-epithelialized and replaced by new tissue, the FBR results in the formation of a collagenous capsule that has a unique appearance and properties.

Implantation of polyvinyl alcohol (PVA) sponges has been adopted as a model for the accurate quantification of angiogenic and fibrogenic responses, as they may occur during wound healing, *in vivo*.[8–11] As an experimental system, the formation of sponge granulomas provides an environment of defined dimensions that is conducive to the invasion of various repair cells and the *de novo* formation of tissue. The system is also preferred when the influence of additional factors, such as epithelial cells, specialized structures including hair follicles and sweat glands, and the process of wound contraction is unnecessary. However, PVA sponges differ from wound healing in that they become encapsulated and elicit the formation of fused macrophages known as foreign body giant cells (FBGCs).[12] FBGCs can secrete a number of cytokines that can influence both the angiogenic and fibrogenic responses. Thus, extrapolation of results obtained from the analysis of sponge granuloma formation to wound healing should be made with caution.

We postulated that, because TSP2 had been shown to modulate both wound healing and the FBR, it would be of interest to analyze the formation of sponge granulomas. In addition, this system could allow for more accurate quantification of the invading tissue. Overall, our studies focused on the effects of the TSP2 deficiency on sponge invasion, including the FBR elicited by the sponge.

New studies have generated increased interest in the mechanisms of action of the TSPs. On one hand, it has been demonstrated that both TSP1 and TSP2 can interact with, and modulate the levels, of matrix metalloproteinases (MMPs).[4,13–15] On the other hand, studies have shown that the proposed ability of TSP1 to modulate the activation of latent transforming growth factor (TGF)-β_1 may not be a major determinant of its activation.[16,17] These findings seem to be inconsistent with the demonstration that the lack of TSP1-mediated activation of TGF-β_1 is a major factor in the development of the TSP1-null phenotype.[18] Based on the identified interaction sites between TSP1 and TGF-β_1 it has been suggested that TSP1 and TSP2 may compete for binding to latent TGF-β_1, but only binding of TSP1 would lead to its activation.[19,20] In this study we addressed these issues by analyzing the deposition of MMP2 and the levels of active TGF-β_1.

Our results demonstrate that, in TSP2-null mice, the process of sponge granuloma formation is altered in a manner similar to wound healing and the FBR. Specifically, we show that matrix remodeling and angiogenesis are affected, and suggest that these changes are because of, in part, changes in MMP2 deposition but not to changes in TGF-β_1 activity. It is apparent from this study that a deficiency in ECM-associated TSP2 can affect repair processes in a complex manner.

Materials and Methods

Animal Model

Generation of TSP2-null mice has been described.[3] In this study we used mice of the C57BL/6/129 SvJ background. All mice were ~16 weeks of age and the same number of male and female animals were used for each genotype.

Grade 3 PVA sponges (M-PACT, Eudora, KA; 3-mm thick and 12-mm diameter) were sterilized under UV light and soaked in endotoxin-free phosphate-buffered saline for 48 hours. Implantations were performed under anesthesia as described previously.[7] Briefly, animals were prepped and two sponges per mouse were implanted subcutaneously in the dorsum through a 1-cm midline incision. Implantation pockets were prepared with the aid of blunt-end butterfly forceps. Incisions were closed with sterile surgical staples. All animals were housed individually for the duration of the experiment.

Sponges were excised *en bloc* at selected time points, photographed, and fixed in 10% zinc-buffered formalin (Anatech, Battle Creek, MI). After processing, the sponges were embedded in paraffin and sectioned (5-μm thick). Sections were then analyzed by histology and immunohistochemistry.

To obtain sponge fluid, excised sponges were cleaned of surrounding tissue and fluid was aspirated by inserting a 26-gauge needle into the sponge. To optimize recovery, sponges were subsequently subjected to centrifugation (10,000 rpm) in a microcentrifuge tube whose top and bottom compartments were separated by a filter.

Sponge fluid was collected from the lower compartment. In initial experiments we did not observe a difference between the needle aspirates and the centrifuged samples. Thus, in all subsequent experiments, sponge fluids were combined before analysis.

Histology, Invasion, and Encapsulation

Sections were stained with hematoxylin and eosin (H&E) according to a standard protocol. The amount of invasion and encapsulation was calculated from micrometer measurements performed independently by two investigators in a blind manner. Fine and dense sponge invasions were defined as described previously.[21] In general, the area of transition from dense to fine invasion was easily detectable. Sponge encapsulation was estimated as described previously for silicone disks.[7] To minimize errors, only the area of the capsule that bordered sponge material was measured. Areas that included sponge openings (pores) were not included in the measurements. Unless otherwise stated, for each time point a total of three sponges (three individual mice) per genotype were examined.

Immunohistochemistry

Sections were stained with antibodies to TSP2,[22] PECAM-1 (Pharmingen, La Jolla, CA), active TGF-β_1 (catalog no. G1221; Promega, Madison, WI), and MMP2 (Chemicon, Temecula, CA). Anti-TSP2 antibody was used as described previously[22] with the following modification. We have found that the immunoreactivity of TSP2 in paraffin-embedded tissues is enhanced after pretreatment of sections with 0.025% pronase for 10 minutes at 37°C. Anti-TGF-β_1, PECAM-1, and MMP2 antibodies were used according to the supplier's instructions. According to the supplier, the anti-TGF-β_1 antibody is highly specific for the active form of the cytokine.

Histomorphometry

Images were captured with the aid of a Photometrics digital camera and analyzed using Metamorph (Universal Image Corporation, Westchester, PA) software. For evaluating angiogenesis, PECAM1-positive vascular profiles were outlined and the collected data including vessel number, vessel size (area and diameter), and the percentage of the image area occupied by vessels were determined by the software. The intrasample vessel diameter distribution was also determined. Angiogenesis was measured only in areas of dense tissue invasion. Areas invaded by fine tissue did not exhibit well-defined vascular profiles with lumens.

For the histomorphometric analysis of MMP2 and active TGF-β_1 levels, a threshold was set representing the maximum background intensity observed in control (no primary antibody) sections. The values obtained represent the relative levels above background for each antibody. Only sections that were stained in the same experiment were used in direct comparisons. This was because of variability in the background levels between

Figure 1. PVA sponges in TSP2-null mice induce excessive fibrosis. PVA sponges were excised *en bloc* 21 days after implantation and photographed. Sponges recovered from TSP2-null mice ($-/-$, **right**) were coated with excess fibrous tissue obscuring the sponge material. On the contrary, less fibrosis was elicited by control sponges and the sponge material was visible ($+/+$, **left**).

experiments. All images were collected in a blind manner, and the scoring of images was performed independently by two investigators.

Assay for Active TGF-β_1

The levels of active TGF-β_1 in sponge fluid, skin extracts, and fibroblast-conditioned media was determined by the PAI-1/luciferase assay for TGF-β using mink lung epithelial cells (clone 32), as described previously.[23] Assay specificity was confirmed by utilization of neutralizing anti-TGF-β_1 antibodies. All comparisons between genotypes were made based on samples containing equal amounts of protein, as determined by the bicinchoninic acid assay (Pierce, Rockford, IL). Fibroblast-conditioned media were harvested from the same passage cells, plated at equal density. Cells were cultured in serum-free media 3 hours before sampling. Equal amounts of skin biopsies, based on weight, were extracted in RIPA buffer.

Statistical Analysis

All differences between data sets were determined by the Student's *t*-tests. Significance required a *P* value of 0.05 or less.

Results

Abnormal Reaction to Sponge and Granuloma Formation in TSP2-Null Animals

Sponges were excised 7, 14, and 21 days after implantation. Explants from TSP2-null and control mice had a similar appearance on both days 7 and 14. On the contrary, day 21 samples differed, as the TSP2-null-derived explants displayed significant fibrosis and hemorrhage (Figure 1, right). Because of the presence of excess tissue and blood the sponge itself was not visible. Instead, the implant was surrounded by a visible fibrous capsule that could not be dissected from the sponge. Control samples did not display significant fibrosis and the sponge could be easily detected by its foam-like appearance (Figure 1, left).

Consistent with our gross observations, differences in the histological appearance of sponge granulomas were

readily apparent only in day 21 explants (Figure 2, C and F). Morphological analysis of the invading response was performed on H&E-stained sections. At day 7, the earliest time point examined, we observed the formation of an organized matrix network within the interstices of the sponge (Figure 2, A and D). This network consisted of areas defined by a fiber-like ECM that resembled a web or net. This interstitial matrix was defined by fibers (arrowheads) at the outer edges, and was subdivided by thin inner fibers (arrows). The term fibrovascular bundles has been used to describe the appearance of this tissue and is considered to be fine invasion.[21] Fine invasion was devoid of mature blood vessels with lumens. Immunohistochemical analysis of day 7 sections revealed that these fibrovascular bundles included fibronectin and von Willebrand factor (data not shown). Overall, day 7 sponges were dominated by fine invasion.

By day 14, numerous invading cells could be observed and the fiber-like ECM network was modified to resemble granuloma (Figure 2, B and E). The appearance of invading tissue was dense and consisted of fibroblast-like cells, ECM, and vessels with lumens. Dense and fine invasion occupied approximately equal areas of the outer and inner parts of the sponge, respectively. TSP2-null-derived granulomas displayed increased staining suggesting increased fibrosis and somewhat increased vascular density. However, the differences between TSP2-null and control were not pronounced. On the contrary, by day 21 the differences between the two genotypes were more obvious. TSP2-null-derived sponges (Figure 2F) exhibited fibrogenic and angiogenic responses that exceeded control (Figure 2C). These differences were obvious as the staining intensity and overall neovascularization of the invading response were increased. The latter was confirmed by histomorphometric analysis after immunolocalization of blood vessels with the endothelial cell marker PECAM1 (see below and Figure 4). The invasion in day 21 sponges was dominated by dense invasion, with only the most inner parts of the sponge displaying fine invasion.

We were also able to observe the formation of numerous FBGCs on the surfaces of the sponge. The FBGCS were present as early as day 7 and increased in number as granuloma formation progressed. No differences in FBGC formation between TSP2-null and control sponges were observed (data not shown).

Table 1. Sponge Invasion and Encapsulation

Genotype	Invasion (μm)	Encapsulation (μm)
TSP2 +/+	270 ± 22	65 ± 20
TSP2 −/−	205 ± 26*	110 ± 18*

Sponges were implanted subcutaneously in mice. After a 3-week implantation period, the implants were explanted, and the degree of dense tissue invasion and sponge encapsulation were determined with the aid of a microscope micrometer. Values shown represent the means of 60 measurements ± 1 SD. A total of six sponges per genotype were evaluated.

*, *P* values ≤ 0.05.
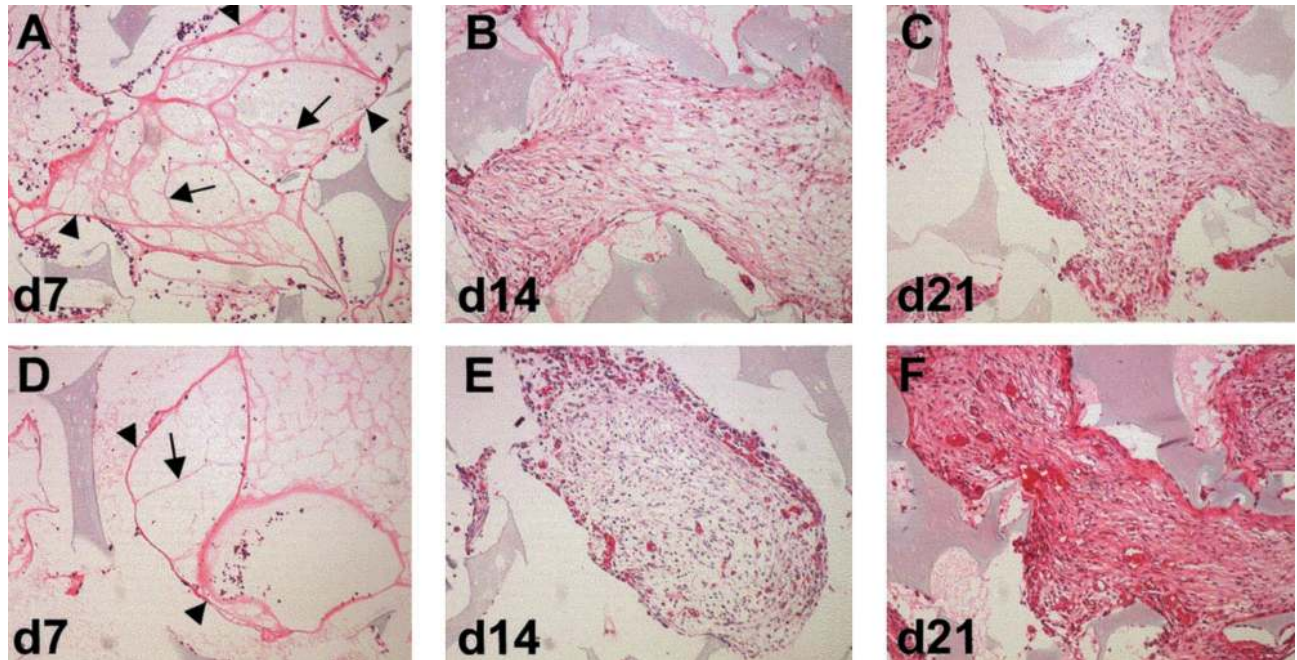
Figure 2. Increased neovascularization and tissue density in TSP2-null animals. Shown are representative sections of PVA sponge implants recovered at 7 (**A**, **D**), 14 (**B**, **E**), and 21 (**C**, **F**) days from control (**A–C**) and TSP2-null (**D–F**) mice and stained with H&E. Fine invasion (d7) characterized by thick (**arrowheads**) and thin (**arrows**) fibrovascular bundles was similar in both genotypes (**A**, **D**). Dense invasion was characterized by increased angiogenesis and tissue density in TSP2-null animals (**E**, **F**). Differences between genotypes were more pronounced at 21 days (compare **C** and **F**). Original magnifications, ×100.

Decreased Sponge Invasion and Increased Encapsulation in TSP2-Null Mice

Quantification of the degree of sponge invasion and encapsulation at day 21 also revealed differences between TSP2-null and control animals (Table 1). Formation of dense tissue did not reach the deep inner crevices of the sponge in TSP2-null animals. On the contrary, sponges in control animals exhibited more pronounced dense invasion. However, despite the reduced migration, the overall
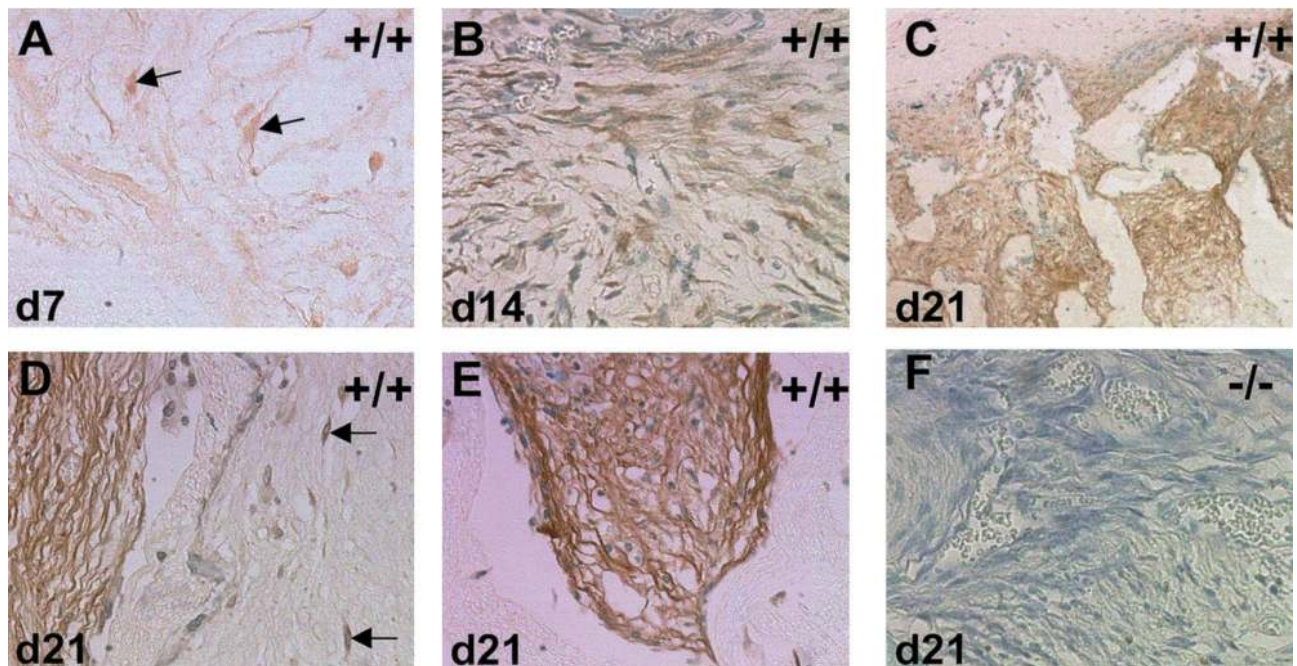
Figure 3. Immnunolocalization of TSP2 in wild-type sponges. Sections from day 7 (**A**), day 14 (**B**), and day 21 (**C–E**) were stained with an anti-TSP2 antibody and visualized by the peroxidase method. At day 7, TSP2 was localized to a few cells (**arrows** in **A**) with fibroblast-like elongated morphology. At day 14 (**B**), TSP2 was also deposited in the ECM, but not extensively. At day 21 (**C–E**), TSP2 was prominent in the both cells and the ECM, with the latter showing strong immunoreactivity. Surrounding foreign body capsules did not exhibit strong ECM-associated TSP2 immunoreactivity (**C**, **D**). Rather, TSP2 deposition was limited to cells (**arrows** in **D**). No immunoreactivity was detected in sections from TSP2-null sponges (**F**; negative control). Original magnifications: ×100 (**C**); ×400 (**A**, **B**, **D–F**).

density of invading tissue was increased in TSP2-null animals. This was apparent after staining of representative sections with H&E (Figure 2, compare C and F) and mirrored previous findings after staining of sections with Masson's trichrome.[24]

Consistent with our previous findings during the FBR, we found that PVA sponges in TSP2-null animals were encapsulated by significantly thicker capsules (Table 1). This finding is also consistent with the superficial appearance of TSP2-null-derived sponges that were surrounded by an excessively fibrous coat (Figure 1). Capsule neovascularization in TSP2-null animals was also increased, more so in day 21 sponges (data not shown).

Spatiotemporal Deposition of TSP2

Immunohistochemical analysis of TSP2 deposition revealed the presence of the protein at all of the time points examined. At day 7, TSP2 seemed to be mostly cell-associated (Figure 3A, arrows) with minimal ECM deposition. At day 14, TSP2 was still predominantly cell-associated, but its deposition in the matrix was increased (Figure 3B). By day 21 we observed a dramatic increase in the deposition of TSP2, especially in the ECM (Figure 3; C to E). Interestingly, TSP2 was abundantly deposited in the sponge granuloma but not in the adjacent developing foreign body capsule (Figure 3, C and D). In the latter, TSP2 was only associated with fibroblast-like cells in the capsule (Figure 3D). On the other hand, deposition in the granuloma was widespread including dense and loose fibers and cells (Figure 3, D and E). No immunohistochemical stain was observed in sponges implanted in TSP2-null animals (Figure 3F; negative control).

Increased Angiogenesis in Sponges Implanted in TSP2-Null Mice

Vascular profiles were visualized by antibodies to the endothelial cell marker PECAM1. Images obtained from areas of the sponge displaying dense granuloma formation were analyzed by histomorphometry. Because of limited dense granuloma formation in day 7 samples, we were unable to estimate their vascularity. Analysis of day 14 and day 21 samples revealed significant differences in the number of blood vessels and the overall vascularity between TSP2-null and control animals (Figure 4). The number of vascular profiles was increased in TSP2-null animals at day 14 and remained high at day 21 (Figure 4, B and C). We observed an overall decrease in vascular density (number of blood vessels and area occupied by blood vessels) as granuloma formation progressed (Figure 4, C and E). The vessel size distribution however, was highly variable and did not differ significantly between genotypes (Figure 4, D and F). Overall, vessel morphology appeared normal (Figure 4, A and B).

### Modulation of TGF-β_1 Activation Is Not Altered in TSP2-Null Mice

The proposed ability of TSPs to modulate TGF-β_1 activity coupled with the increased fibrotic response in TSP2-null mice suggested that the levels of this growth factor might be elevated. Histomorphometric semiquantitative analysis of representative sections stained with anti-active TGF-β_1 antibodies revealed no significant differences between TSP2-null and control animals (data not shown). Levels of active TGF-β_1 were highest at day 14, but dropped close to background by day 21. For more accurate quantification, we collected sponge fluid from day 14 sponges and measured active TGF-β_1 by the PAI-1/luciferase assay. No significant differences between TSP2-null and control samples were observed (Table 2). Furthermore, similar results were obtained from the analysis of skin extracts and the conditioned media of dermal fibroblasts (Table 2).

Increased MMP2 Deposition in the ECM of TSP2-Null Mice

Imunohistochemical analysis of MMP2 distribution in dense tissue in day 14 and day 21 implants revealed significant differences between TSP2-null and control animals (Figure 5). During both time points, the distribution of MMP2 in TSP2-null-derived sponges appeared to be more widespread, displaying a significant association with both cells and the ECM (Figure 5, C and D; arrows and asterisks). On the contrary, MMP2 deposition in control sponges was predominantly associated with cells (Figure 5, A and B; arrows) and did not seem to be extensively associated with the matrix (Figure 5, A and B; asterisks). Histomorphometric analysis of sections stained with anti-MMP2 antibodies revealed that TSP2-null sponges displayed a twofold increase in the levels of MMP2, mirroring its extensive distribution (Figure 5E). No decrease in the levels of MMP2 between day 14 and day 21 were observed. Deposition of MMP2 in surrounding capsules was predominantly cell-associated at day 14 and day 21 in both genotypes. No significant differences in its deposition between genotypes were observed (data not shown).

Discussion

TSP2, as a matricellular protein, has been proposed to function, in part, by modulating the availability of proteases and growth factors.[1] Thus, its presence in the ECM, coupled with its ability to interact with specific cell-surface receptors, enables the ECM to modulate processes such as angiogenesis and matrix remodeling. A number of observations made in TSP2-null mice suggest a role for TSP2 in both processes.[3,6,7] For example, collagen fibers and fibrils appear disorganized in TSP2-null mice, with the latter displaying abnormal shape and size.[3] In addition, abnormalities have been observed in the interaction of newly secreted collagen fibrils with the
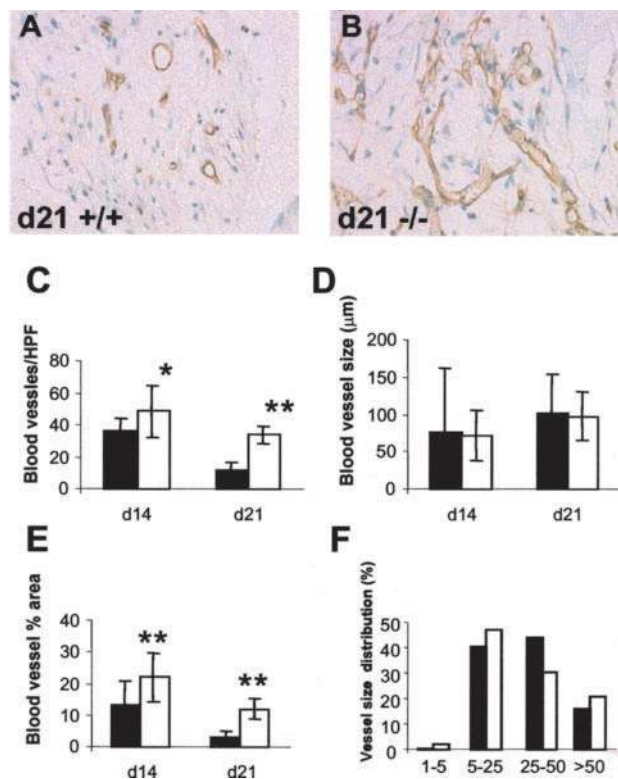
Figure 4. Increased angiogenesis in TSP2-null sponges. **A** and **B**: Sections from day 21 sponges from control (**A**) and TSP2-null (**B**) mice were stained with an anti-PECAM1 antibody and visualized by the peroxidase method. An increased number of vascular profiles can be seen in TSP2-null sponges (**B**). Original magnifications, ×400. **C–F:** Computer-assisted vessel quantification in day 14 and day 21 sponges from control (**solid bars**) and TSP2-null (**open bars**) mice. An increased number of vascular profiles per high-power field (0.04 μm^2) was observed in TSP2-null sponges (**C**), resulting in an overall increase in the percentage of the field occupied by vessels (**E**). Vessel size and size distribution were similar (**D**, **F**). *, $P \leq 0.05$; **, $P \leq 0.005$.

Figure 5. ECM-associated MMP2 is increased in TSP2-null mice. **A–D:** Sections from day 14 (**A**, **C**) and day 21 (**B**, **D**) sponges from control (**A**, **B**) and TSP2-null (**C**, **D**) mice were stained with an anti-MMP2 antibody and visualized by the peroxidase method. **Arrows** and **asterisks** denote immunoreactive cells and matrix, respectively. Increased MMP2 deposition in the ECM was evident in TSP2-null sections (**C**, **D**). Original magnifications, ×400. **E:** Histomorphometric quantification of MMP2 deposition. Relative levels of MMP2 at day 14 and day 21 in sponges of control (**solid bars**) and TSP2-null (**open bars**) mice. Values are arbitrary units. *, $P \leq 0.05$.
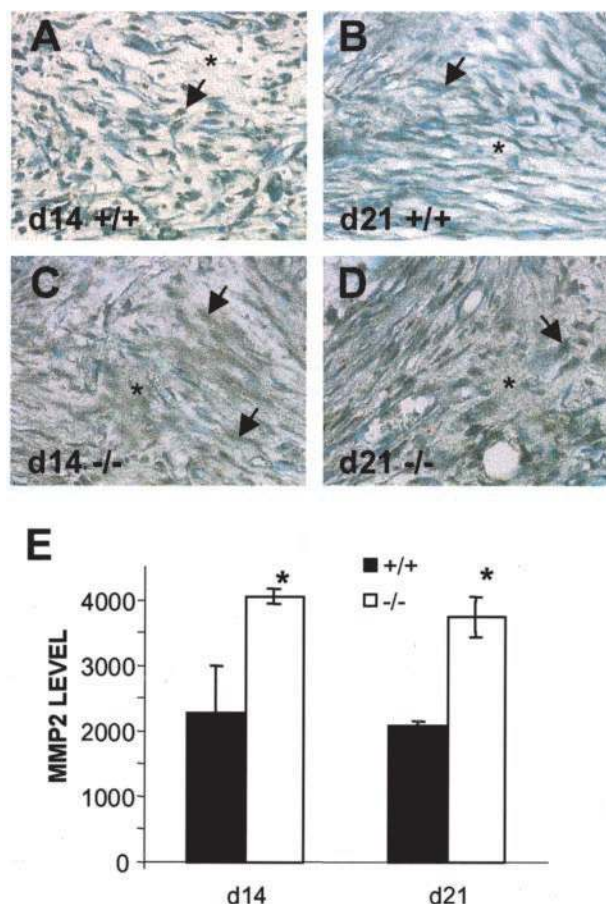
cellular processes of tendon fibroblasts in newborn mice.[24] As a consequence, the ability of fibrils to organize into fibers was compromised. The exact mechanism that leads to the development of these abnormalities remains unclear. We have suggested that it may be linked to the adhesive defect of TSP2-null fibroblasts, which we have shown to be related to increased levels of MMP2.[4,15]

In this study, we show that a deficiency in TSP2 influences intermediate and late events during sponge gran-

Table 2. Active TGF-β_1 Levels (pM) in Control and TSP2-Null Animals

	TSP2+/+	TSP2−/−
Sponge fluid (day 14)	1.14 ± 0.21	0.85 ± 0.33
Skin (12 weeks)	1.51 ± 0.34	1.15 ± 0.31
Skin fibroblasts	6.55 ± 3.12	4.18 ± 3.46

Sponges were implanted subcutaneously in mice. After a 2-week period, the implants were explanted, and the levels of active TGF-β_1 in sponge fluid were determined by the PAI-1/luciferase assay. Skin was removed from adult mice and either extracted for determination of active TGF-β_1 levels, or processed for isolation of fibroblasts. Conditioned media from fibroblasts grown in culture were harvested and the levels of active TGF-β_1 were determined. A total of three sponges, three skin samples, and fibroblast cultures from three individual mice per genotype were analyzed.

uloma formation. Thus, the observed abnormal matrix deposition and increased and prolonged angiogenesis coincided with the deposition of TSP2 within the ECM of wild-type sponges. On the contrary, during the early phase of granuloma formation, when TSP2 deposition was not associated with the ECM but was only limited to a few fibroblast-like cells, no abnormalities were observed. These findings are consistent with our previous analysis of healing cutaneous wounds.[6] In this repair model, we observed that the effect of TSP2 deficiency was amplified in the period during which TSP2 would be expected to associate extensively with the ECM.

It is clear from this study, and the analysis of wound healing and the FBR, that TSP2 deficiency results in increased and prolonged neovascularization of the newly formed tissue. Because of the increased vascular density of dermis and adipose tissue that are proximal to the sponge, we postulated that a higher number of blood vessels would invade the sponge in TSP2-null mice. Our findings however, show that differences in granuloma neovascularization become more pronounced in the late phase of the response. This finding indicates that the

initial invasion of the sponge does not significantly differ between wild-type and TSP2-null mice. Rather, it suggests that changes in sponge neovascularization are primarily because of a TSP2 deficiency within the remodeling granuloma. Supporting evidence for this hypothesis has been obtained from studies demonstrating that delivery of anti-sense TSP2 DNA to sponges in wild-type mice can result in increased neovascularization.[34] Thus, sponge angiogenesis can be altered without a change in the vascular density of surrounding tissues.

Despite the extensive documentation of the anti-angiogenic activity of TSP2, the exact mechanism of inhibition remains uncertain.[1,2] It has been shown that TSP1 can induce endothelial cell apoptosis in culture and in the blood vessels of sponges and experimental tumors.[25–27] Furthermore, it has been shown that apoptosis is induced after the interaction of TSP1 with the scavenger receptor CD36 leading to downstream activation of the caspase pathway .[26,27] It is tempting to assume that, because the TSP1-CD36-binding site is conserved in TSP2, the same mechanism may be at play in this and other tissue repair systems. However, because of their distinct spatiotemporal distribution, TSP1 and TSP2 may not perform similar functions. For example, immunohistochemical analysis of healing wounds revealed minimal overlap in the deposition of TSP1 and TSP2.[6] The former was prominent early (day 3) and became undetectable by day 7, whereas the latter appeared later (days 3 to 5) and peaked at day 10. Because maximal vascular regression in healing wounds occurs at day 10, we suggest that TSP2 and not TSP1 is the major determinant of angiogenesis during repair. Whether TSP2 functions by inducing apoptosis in endothelial cells could be addressed by determining the number of cells undergoing apoptosis in the wounds of TSP2-null mice. It should be noted however, that the presence of an alternative vascular regression mechanism has been suggested from the ultrastructural analysis of long-term (100 to 130 days) collagen sponge implants in the rat.[28] In this study, degenerating endothelial cells, not undergoing apoptosis, could be identified on the basis of nuclear morphology.

TSP2 may also influence angiogenesis indirectly, by modulating the availability of MMP2, as has been suggested by *in vitro* studies. MMPs have active roles during matrix remodeling and other tissue regeneration processes, including modulation of angiogenesis.[29–31] Numerous studies have implicated MMP2 and its inhibitor TIMP-2 in the process of wound healing.[32,33] In this study we observed that both TSP2 and MMP2 are located in the ECM at day 14 and day 21, suggesting that an interaction between the two may be possible. Indeed, our results demonstrate increased MMP2 deposition in the ECM of sponge granulomas of TSP2-null animals. By semiquantitative histomorphometry we were able to show that the increase is in the twofold range, similar to that observed in cultured fibroblasts. Validation of the histomorphometric quantification has been achieved by analysis of cutaneous wounds. In this system, a twofold to threefold increase in the levels of MMP2 in TSP2-null animals was observed both by histomorphometry and zymography (T. R. Kyriakides, A. Agah, and P. Bernstein, manuscript in preparation). The latter method can provide sensitive and reliable quantification of MMPs. Based on the changes in the deposition of MMP2, we postulate that a TSP2-MMP2 interaction within the ECM is critical to the processes of synthesizing and remodeling matrix, and to neovascularization during repair.

In this study we also investigated the possibility that a deficiency in TSP2 could affect activation of TGF-β_1. By using histomorphometry and the PAI-1/luciferase assay we were unable to observe any significant changes in the levels of active TGF-β_1 in the sponges of TSP2-null mice. We extended our studies to include analysis of skin extracts and primary dermal fibroblasts grown in culture. The latter is considered to mimic stress conditions because the cells are placed in a serum-rich environment.[4] In both cases we were unable to detect any changes in the levels of active TGF-β_1 between control and TSP2-null samples. Thus, the increased fibrosis observed within and surrounding the sponges in TSP2-null mice may not be associated with elevated levels of TGF-β_1. Our findings in cultured cells are not unexpected because we had not observed an increase in collagen synthesis, as one would expect from increased TGF-β_1 activity, in TSP2-null fibroblasts.[3] Based on our findings, we suggest that TSP2 does not play a significant role in modulating the activity of TGF-β_1 in culture or during tissue repair and regeneration. However, it should be emphasized that our *in vivo* investigation has been limited to selected time points. Conceivably, TGF-β_1 activity may be modulated by TSPs at intervals that we have not examined. Furthermore, modulation of TGF-β_1 activity by TSP2 may be at levels below the detection limit of our assay. This issue can be addressed by analysis of more time points and by using more sensitive assays (eg, enzyme-linked immunosorbent assay).

Based on the ability of TSP2-null wounds to heal with reduced scarring and the increased vascularity of capsules, we proposed that TSP2 may serve as a molecular target whose inhibition could lead to improved healing.[1] In fact, we have recently shown that inhibition of TSP2 synthesis by local administration of antisense TSP2 cDNA reproduced the TSP2-null phenotype in wild-type and TSP2-null animals.[34] Specifically, we were successful in increasing sponge neovascularization. We are currently planning studies designed to test the functional significance of the increased sponge neovascularization in TSP2-null animals.

Acknowledgments

References

1. Bornstein P: Thrombospondins as matricellular modulators of cell function. J Clin Invest 2001, 107:929–933
2. Lawler J: The functions of thrombospondin-1 and -2. Curr Opin Cell Biol 2000, 12:634–640

3. Kyriakides TR, Zhu YH, Smith LT, Bain SD, Yang Z, Lin MT, Danielson KG, Iozzo RV, LaMarca M, McKinney CE, Ginns EI, Bornstein P: Mice that lack thrombospondin 2 display connective tissue abnormalities that are associated with disordered collagen fibrillogenesis, an increased vascular density, and a bleeding diathesis. J Cell Biol 1998, 140:419–430

4. Yang Z, Kyriakides TR, Bornstein P: Matricellular proteins as modulators of cell-matrix interactions: adhesive defect in thrombospondin 2-null fibroblasts is a consequence of increased levels of matrix metalloproteinase-2. Mol Biol Cell 2000, 11:3353–3364

5. Hankenson KD, Bain SD, Kyriakides TR, Smith EA, Goldstein SA, Bornstein P: Increased marrow-derived osteoprogenitor cells and endosteal bone formation in mice lacking thrombospondin J Bone Miner Res 2000, 15:851–862

6. Kyriakides TR, Tam JW, Bornstein P: Accelerated wound healing in mice with a disruption of the thrombospondin 2 gene. J Invest Dermatol 1999, 113:782–787

7. Kyriakides TR, Leach KJ, Hoffman AS, Ratner BD, Bornstein P: Mice that lack the angiogenesis inhibitor, thrombospondin 2, mount an altered foreign body reaction characterized by increased vascularity. Proc Natl Acad Sci USA 1999, 96:4449–4454

8. Fajardo LF, Kowalski J, Kwan HH, Prionas SD, Allison AC: The disc angiogenesis system. Lab Invest 1988, 58:718–724

9. Davidson JM, Klagsbrun M, Hill KE, Buckley A, Sullivan R, Brewer PS, Woodward SC: Accelerated wound repair, cell proliferation, and collagen accumulation are produced by a cartilage-derived growth factor. J Cell Biol 1985, 100:1219–1227

10. Andrade SP, Fan TP, Lewis GP: Quantitative in-vivo studies on angiogenesis in a rat sponge model. Br J Exp Pathol 1987, 68:755–766

11. Sephel GC, Kennedy R, Kudravi S: Expression of capillary basement membrane components during sequential phases of wound angiogenesis. Matrix Biol 1996, 15:263–279

12. Or R, Feferman R, Shoshan S: Thalidomide reduces vascular density in granulation tissue of subcutaneously implanted polyvinyl alcohol sponges in guinea pigs. Exp Hematol 1998, 26:217–221

13. Qian X, Wang TN, Rothman VL, Nicosia RF, Tuszynski GP: Thrombospondin-1 modulates angiogenesis in vitro by up-regulation of matrix metalloproteinase-9 in endothelial cells. Exp Cell Res 1997, 235:403–412

14. Bein K, Simons M: Thrombospondin type 1 repeats interact with matrix metalloproteinase 2. Regulation of metalloproteinase activity. J Biol Chem 2000, 275:32167–32173

15. Yang Z, Strickland DK, Bornstein P: Extracellular MMP2 levels are regulated by the LRP scavenger receptor and thrombospondin 2. J Biol Chem 2001, 276:8403–8408

16. Abdelouahed M, Ludlow A, Brunner G, Lawler: Activation of platelet-transforming growth factor beta-1 in the absence of thrombospondin-1. J Biol Chem 2000, 275:17933–17936

17. Grainger DJ, Frow EK: Thrombospondin 1 does not activate transforming growth factor beta1 in a chemically defined system or in smooth-muscle-cell cultures. Biochem J 2000, 350:291–298

18. Crawford SE, Stellmach V, Murphy-Ullrich JE, Ribeiro SM, Lawler J, Hynes RO, Boivin GP, Bouck N: Thrombospondin-1 is a major activator of TGF-beta1 in vivo. Cell 1998, 93:1159–1170

19. Schultz-Cherry S, Chen H, Mosher DF, Misenheimer TM, Krutzsch HC, Roberts DD, Murphy-Ullrich JE: Regulation of transforming growth factor-beta activation by discrete sequences of thrombospondin 1. J Biol Chem 1995, 270:7304–7310

20. Murphy-Ullrich JE, Poczatek M: Activation of latent TGF-beta by thrombospondin-1: mechanisms and physiology. Cytokine Growth Factor Rev 2000, 11:59–69

21. Reed MJ, Corsa A, Pendergrass W, Penn P, Sage EH, Abrass IB: Neovascularization in aged mice: delayed angiogenesis is coincident with decreased levels of transforming growth factor beta1 and type I collagen. Am J Pathol 1998, 152:113–123

22. Kyriakides TR, Zhu YH, Yang Z, Bornstein P: The distribution of the matricellular protein thrombospondin 2 in tissues of embryonic and adult mice. J Histochem Cytochem 1998, 46:1007–1015

23. Abe M, Harpel JG, Metz CN, Nunes I, Loskutoff DJ, Rifkin DB: An assay for transforming growth factor-beta using cells transfected with a plasminogen activator inhibitor-1 promoter-luciferase construct. Anal Biochem 1994, 216:276–284

24. Bornstein P, Kyriakides TR, Yang Z, Armstrong LC, Birk DE: Thrombospondin 2 modulates collagen fibrillogenesis and angiogenesis. J Invest Dermatol Symp Proc 2000, 5:61–66

25. Guo N, Krutzsch HC, Inman JK, Roberts DD: Thrombospondin 1 and type I repeat peptides of thrombospondin 1 specifically induce apoptosis of endothelial cells. Cancer Res 1997, 57:1735–1742

26. Jimenez B, Volpert OV, Crawford SE, Febbraio M, Silverstein RL, Bouck N: Signals leading to apoptosis-dependent inhibition of neovascularization by thrombospondin-1. Nat Med 2000, 6:41–48

27. Nor JE, Mitra RS, Sutorik MM, Mooney DJ, Castle VP, Polverini PJ: Thrombospondin-1 induces endothelial cell apoptosis and inhibits angiogenesis by activating the caspase death pathway. J Vasc Res 2000, 37:209–218

28. Honma T, Hamasaki T: Ultrastructure of blood vessel regression in involution of foreign-body granuloma. J Submicrosc Cytol Pathol 1998, 30:31–44

29. Werb Z, Vu TH, Rinkenberger JL, Coussens LM: Matrix-degrading proteases and angiogenesis during development and tumor formation. APMIS 1999, 107:11–18

30. Parks WC: Matrix metalloproteinases in repair. Wound Repair Regen 1999, 7:423–432

31. Ravanti L, Kahari V: Matrix metalloproteinases in wound repair. Int J Mol Med 2000, 6:391–407

32. Inkinen K, Turakainen H, Wolff H, Ravanti L, Kahari VM, Ahonen J: Expression and activity of matrix metalloproteinase-2 and -9 in experimental granulation tissue. APMIS 2000, 108:318–328

33. Madlener M, Parks WC, Werner S: Matrix metalloproteinases (MMPs) and their physiological inhibitors (TIMPs) are differentially expressed during excisional skin wound repair. Exp Cell Res 1998, 242:201–210

34. Kyriakides TR, Hartzel T, Huynh G, Bornstein P: Regulation of angiogenesis and matrix remodeling by localized, matrix-mediated antisense gene delivery. Mol Ther 2001, 3:842–849